# ChemComm

Accepted Manuscript


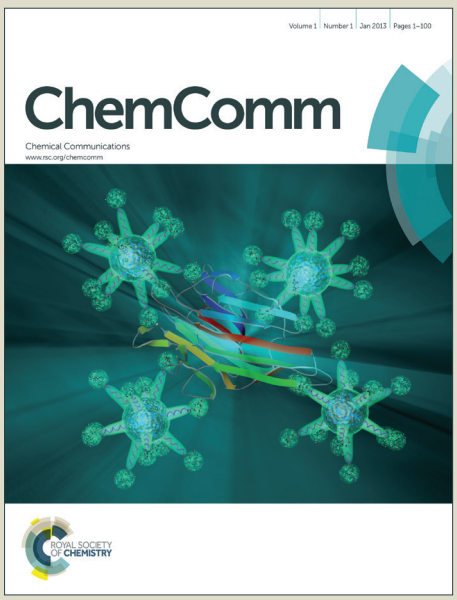





ROYAL SOCIETY OF CHEMISTRY

www.rsc.org/chemcomm

Cite this: DOI: 10.1039/c0xx00000x

www.rsc.org/xxxxxx

ARTICLE TYPE

# Highly Sensitive Turn-on Biosensors by Regulating Fluorescence Dye Assembly on Liposome Surfaces

**Sungbaek Seo,[a,‡] Min Sang Kwon,[b,‡] Andrew W. Phillips,[a,‡] Deokwon Seo,[b] and Jinsang Kim[a,b,c,d,e,*b]**

***Received (in XXX, XXX) Xth XXXXXXXXX 20XX, Accepted Xth XXXXXXXXX 20XX***

**DOI: 10.1039/b000000x**

**We developed a new self-signaling sensory system built on phospholipid liposomes having H-aggregated R6G dyes on their surface. Selective molecular recognition of a target by the phospholipid displaces R6G from the liposome surface to turn on fluorescence signal. Selective and sensitive detection of neomycin down to 2.3 nM is demonstrated.**

Liposomes are spherical nanostructures consisting of a lipid bilayer surrounding an aqueous core. The unique bilayer architecture, dynamic nature, and functionalizable surface of liposomes provide an important scaffold for drug delivery[1-3] and for various analytical applications.[4-6] An attractive analytical application of liposomes is as a sensor platform for detecting important chemical and biological analytes.[7-9] Amplification of the sensory signal, good biocompatibility, and simple preparation without complex chemical synthesis of liposomes are attractive features for developing liposomes as a sensor platform.[10,11] Liposome-based sensors are typically composed of fluorescence dyes and/or electrochemical markers located in the aqueous core or within the lipid bilayer, with specific receptors conjugated onto the liposome surface.[12-14] When target analytes encounter the system, the receptors interact with the target analytes, thereby triggering the signal-generation mechanism through various signal transduction mechanisms such as liposome collapse, Förster resonance energy transfer (FRET), photoinduced electron transfer (PeT) between dyes and analytes or steric repulsion of analytes for affinochromic polymer liposomes.[15-24] However, dye encapsulation methods suffer from several drawbacks including low loading efficiency, poor control of the amount of encapsulated dyes, and self-quenching of dyes

Herein, we report our systematic approach to develop a novel liposome-based sensing platform from the interesting observation: the fluorescence of Rhodamine 6G (R6G) dyes is efficiently quenched on phospholipid-liposome surfaces. Through thorough investigation of this observation, we revealed the origin of this phenomenon and developed a unique turn-on sensing platform able to detect bioanalytes, neomycin as an example, with very high sensitivity, down to 2.3 nM, one of the most sensitive aminoglycosidic antibiotic detection systems reported among liposome-based sensors.

We illustrated our strategy to realize the liposome-based sensing platform from the observation in Scheme 1. Liposome-R6G complexes used in the detection of target analytes were prepared from the mixed solution of phospholipids and polydiacetylene monomer (PCDA). Specific phospholipids were introduced to the system for selective interaction with target analytes and PCDA monomers are incorporated to enhance the stability of the liposome because PCDA can be photopolymerized. Coulombic interactions between cationic R6G dyes and anionic phospholipids and concomitant hydrophobic interactions of the resulting complexes caused aggregation-induced fluorescence quenching of R6G dyes on phospholipid-liposome surfaces. When the target analytes are added, strong specific interactions between phospholipids and the target analytes break the non-specific Coulombic interactions between R6G dyes and phospholipids, leading to displacement of R6G dyes by the target analytes and subsequent fluorescence recovery as a sensory signal.

When an aqueous solution of 1,2-dimyristoyl-*sn*-glycero-3-phosphate (DMPA; $1 \times 10^{-4}$ M, 20 μl; a chemical structure in **Scheme 2a**) was added to an aqueous solution of R6G ($1 \times 10^{-5}$ M, 1 ml), the fluorescence of R6G was gradually quenched as the amount of DMPA increased (**Figure 1a**). A dramatic change was also observed in the UV-Vis spectrum. The main absorption band at 527 nm progressively decreased and new peaks at around 509 nm and 451 nm appeared (**Figure 1b**). We hypothesized that this interesting R6G quenching originated from the aggregation-induced emission quenching by means of the formation of H-type aggregates of R6G mediated by DMPA.[25-28]

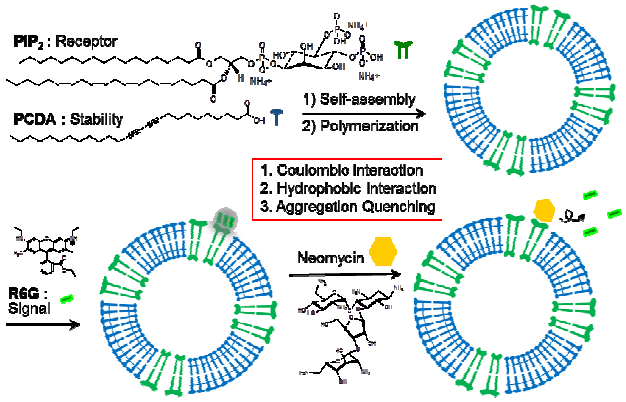


**Scheme 1.** Schematic illustration of the novel liposome-based turn-on sensor design principle. Diacetylene monomers (PCDA) and phospholipids are incorporated into the liposomes to enhance the stability of liposomes and to respond to target analytes, respectively. Rhodamine 6G (R6G) emission is quenched on the liposome surface by the formation of H-aggregates driven by Coulombic interactions between R6G dyes and phospholipids and concomitant hydrophobic interactions of dyes. Specific interaction between target analytes and phospholipids leads to the displacement of R6G dyes in favor of the target analytes, inducing the sensory signal.

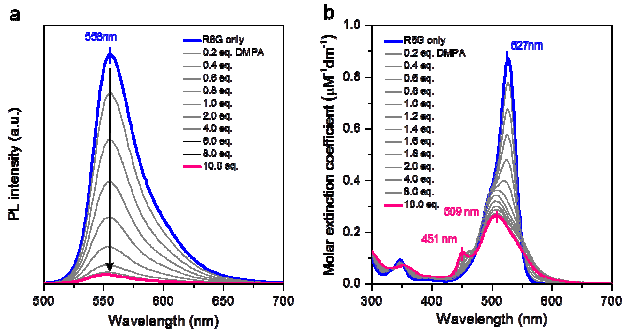


**Figure 1.** (a) Photoluminescence (PL) spectra and (b) UV-Vis absorption spectra of R6G in the presence of DMPA.

We developed the hypothesis based on the structural features of DMPA and R6G. DMPA is a phospholipid comprised of a water-soluble anionic head and two long hydrophobic alkyl tails. Due to this amphiphilic nature, it can readily form liposomes in water above its critical bilayer concentration (CBC).[29] R6G is a moderately water-soluble cationic dye. We assumed that negatively-charged DMPA would attract cationic R6G, triggering aggregation to minimize surface energy of the resulting hydrophobic R6G-DMPA complexes (**Scheme 2a**). Several studies have demonstrated that electrostatic interactions between cationic dyes and negatively-charged colloids such as micelles,[30,31] vesicles,[32] clays,[33] silica,[34,35] and self assembled monolayer-treated gold nanoparticles,[36,37] led to aggregation of dye molecules, supporting our hypothesis.

We carefully compared three different amphiphilc molecules with different charge characteristics to confirm our hypothesis. Positively-charged hexadecyltrimethylammonium bromide (CTAB) and neutral polyoxyethylene (20) sorbitan monolaurate (Tween 20) did not show any signature for R6G aggregation, while negatively charged sodium lauryl sulfate (SDS) generated H-type aggregates of R6G dyes (**Figure S1**). These results clearly indicate that Coulombic interactions play a crucial role in R6G aggregation, as we expected. However, when $KH_2PO_4$ was added to a water solution of R6G, we did not observe R6G aggregation even though $KH_2PO_4$ has a negative charge on its own (**Figure S1**). We attribute this to the absence of long alkyl chains in $KH_2PO_4$. Even if $KH_2PO_4$-R6G complexes form via Coulombic interactions, it is difficult to assemble into aggregates because the resulting $KH_2PO_4$-R6G complexes are quite hydrophilic and stable enough in an aqueous environment.

We investigated the PL quenching ratio of R6G versus DMPA concentration to understand the detailed mechanism of R6G aggregation. The curve in **Scheme 2b** shows a transition point at a very low concentration, 0.002 mM; rapid quenching started from 0.001 mM and saturated at around 0.01 mM. SEM analysis combined with dynamic light scattering study indicates that R6G dyes and DMPA lipids assemble to form spherical nanoparticles, i.e. liposomes, above the CBC and this led to R6G aggregation as well (**Figure S2**). To determine CBC value of DMPA, fluorescence intensities of the peaks at ~375 nm ($I_1$) and ~385 nm ($I_3$) were extracted from the PL spectra (**Figure S3**). The $I_1/I_3$ values were plotted against the serially diluted lipid concentration; the inflection point of this plot is defined as CBC (**Scheme 2b**).[38] Furthermore, the fact that the transition concentration (0.002 mM) of quenching ratio is far below the CBC of DMPA (~0.3 mM) implies that the DMPA-R6G

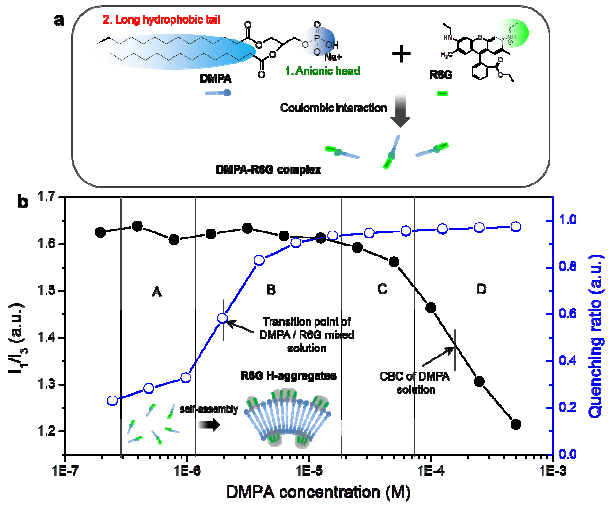


**Scheme 2.** (a) Illustrated scheme of DMPA-R6G complex triggered by Coulombic interactions between anionic DMPA and cationic R6G. (b) Quenching ratio of R6G emission (blue circle) was plotted versus DMPA concentration. CBC value of DMPA was determined by $I_1/I_3$ value (black circle) using pyrene fluorescence probing (see **Figure S3** for details). We illustrated the plausible H-aggregate mechanism of the system in the inset.

complexes resulting from Coulombic interactions are more hydrophobic than pure DMPA and so the complexes can form liposomes even at much lower concentrations of DMPA than the CBC of DMPA. After obtaining a clear picture of the R6G aggregation mechanism through systematic analysis, we further investigated the strength of the Coulombic interactions between DMPA and R6G in an aqueous environment. We calculated the binding constant ($K_b$) through PL titration of an aqueous solution of DMPA with R6G (**Figure S4**). The $K_b$ value was measured to be $6.3\times10^5$ in the presence of 0.1 equiv. of R6G, which is consistent with other reported systems and is strong enough to form DMPA-R6G complexes in water.[39] Interestingly, the measured $K_b$ value decreased as the amount of R6G increased despite the fact that $K_b$ value should be constant, theoretically, implying that R6G already bound to liposome surfaces may interfere with binding of other R6G dyes.

Based on the systematic analysis of this observation, we developed a new sensory platform to detect various bioanalytes. It is well known that phospholipids specifically interact with bioanalytes.[40] We envisioned that the specific interaction between phospholipids and target analytes would break the non-covalent interactions between R6G and phospholipids leading to displacement of R6G dyes by the target analytes and subsequent fluorescence recovery as a fluorescence turn-on sensory signal.

Our initial trial to use R6G-DMPA liposomes as a sensory platform was unsuccessful because the liposomes easily precipitated out of solution in 1-2 days at room temperature (**Figure S5**). To achieve long-term stability and convenient preparation of the liposome solution, we decided to co-assemble diacetylene monomers, which are well-known to accommodate various phospholipids and form stable liposomes.[41,42] Co-assembled liposomes were expected to be easily polymerized by UV light, leading to the enhanced stability of the liposomes in solution. We prepared a co-assembled liposome solution comprised of DMPA-PCDA by following the reported procedure (Note: detailed procedure is also described in the experimental section).[41,42] Subsequent treatment of the co-assembled liposome solution with 254 nm UV-light resulted in polymerized liposomes

as the developed blue color implies. As expected, the resulting liposome solution shows excellent stability without forming aggregation or precipitation for months under ambient conditions.

We examined whether the co-assembled liposomes can still induce the R6G quenching. Addition of R6G dyes into the liposome solution indeed resulted in significant emission quenching of the dyes, which is in accordance with the DMPA-R6G system. Changes in UV-Vis spectrum clearly indicate that R6G dyes form H-type R6G aggregates on the co-assembled liposome surfaces through Coulombic interactions. We calculated the $K_b$ value for the co-assembled liposome through a PL titration (**Figure S6**). Very interestingly, the calculated $K_b$ value was 3 times higher than for that of DMPA-R6G. We assumed that the well-regulated surface of co-assembled liposome would increase $K_b$ value, but do not fully understand the increase in $K_b$ value yet.

We selected neomycin as a target analyte. Neomycin is an aminoglycosidic antibiotic with diverse applications in human and veterinary medicine, particularly in the livestock industry. Due to the ototoxicity and nephrotoxicity of neomycin, there is interest in monitoring the levels of the drug in livestock products. Furthermore, overuse of neomycin contributes to antibiotic-resistant bacteria, providing another motivation to monitor levels of the drug in the food supply. Phosphatidylinositol 4,5-bisphosphate ($PIP_2$), a lipid component of cellular membranes, is part of the inositol 1,4,5-triphosphate / diacylglycerol signal transduction pathway. Normally, $PIP_2$ acts as a substrate for the enzyme phospholipase C, which catalyzes the hydrolysis of the lipid. Neomycin is known to bind $PIP_2$, which inhibits the hydrolysis, and thus the downstream signal cascade.[41]

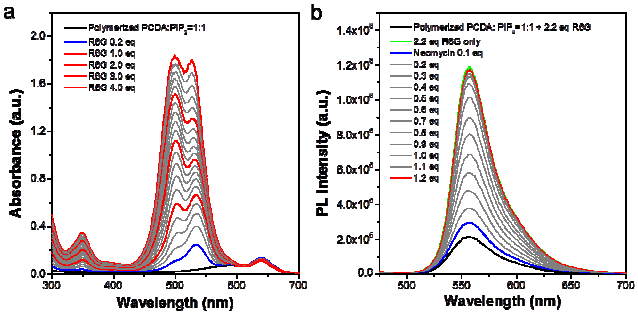


**Figure 2**. (a) UV-Vis absorption spectra of PCDA/$PIP_2$ based liposomes in the presence of different amounts of R6G. (b) Changes in PL spectra of PCDA/$PIP_2$/R6G based liposome sensor by the addition of neomycin.

We prepared an aqueous solution of polymerized co-assembled liposomes (**Figure S7**) comprised of PCDA:$PIP_2$ (1:1, 50 μM). Addition of R6G dye to the liposome solution resulted in significant emission quenching of the dye. The changes in the UV-Vis spectrum clearly indicate that the emission quenching of the dyes is attributed to the formation of H-type aggregates of R6G on liposome surfaces (**Figure 2a**). We calculated the quenching efficiency of R6G dyes for the $PIP_2$-R6G complexes through UV-Vis titration. The maximum quenching of the $PIP_2$-R6G system was observed at 2.2 equivalents of R6G (**Figure 2a**). The formation of H-type aggregates of dyes should theoretically reach the maximum quenching efficiency at 3.0 equivalents of dyes for the $PIP_2$-R6G system because $PIP_2$ contains three phosphate groups (refer the $PIP_2$ structure in **Scheme 1a**). We attributed this difference to the structural features of $PIP_2$, which possesses two external phosphates and one internal phosphate

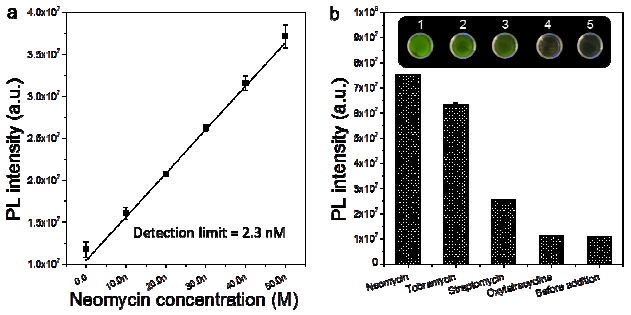


**Figure 3** (a) PL intensity of PCDA/$PIP_2$/R6G based liposome sensor was indicated versus neomycin concentration in the system. Black line shows linear fitting curve. (b) PL intensity of PCDA/$PIP_2$/R6G based liposome sensor was measured in the presence of the same concentration of neomycin (1), tobramycin (2), streptomycin (3), and oxytetracycline (4).

group. The two outside phosphate groups can easily interact with R6G dyes and cause H-aggregates, while the internal phosphate may not able to bind efficiently with dyes due to the large steric hindrance. As shown in Figure S8, addition of neomycin to the PCDA/$PIP_2$ liposome-R6G system restored the shape of the absorption spectra of R6G, but did not change the absorption of the photopolymerized PCDA at around 650 nm meaning that PCDA did not contribute to the optical transition of this sensor system. As the amount of neomycin increased, the emission intensity of R6G gradually increased and it restored the original fluorescence when 1.2 equivalents of neomycin were added (**Figure 2b**), implying that neomycin forms a 1:1 complex with $PIP_2$, which is in good accordance with previous research.[43]

We conducted sensitivity tests with the DI-water solution of neomycin at various concentrations. Distinguishable R6G emission recovery was observed with 2.3 nM neomycin, which is at least 10 times better than the established 0.1 μM of detection limit of neomycin in our previously published system (**Figure 3a**).[44] We stretched our detection study to other aminoglycosidic antibiotics (tobramycin, streptomycin) because $PIP_2$ lipids are known to bind to aminoglycosidic antibiotics including neomycin.[45,46] As predicted, the liposome sensor also generated a certain level of a fluorescence turn-on (**Figure 3b**). The turn-on signal intensity for aminoglycosidic antibiotics showed a trend (neomycin > tobramycin > streptomycin), which is identical to interaction strength of aminoglycosidic antibiotics toward $PIP_2$ in our previous study.[41] However, non-aminoglycosidic antibiotic, i.e., oxytetracycline, having a different chemical structure from the aminoglycosidic antibiotics, did not produce any sensory signals. Since the H-aggregation formation relies on the Coulombic interaction between the R6G and phospholipids, we were concerned that the physiological environment (high ionic strength) would induce the de-quenching of R6G dyes by a charge screening effect, resulting in decreased selectivity. Unfortunately, as we expected, the sensor system showed considerable de-quenching of dyes in PBS buffer condition. To address this matrix effect, we designed a sample-preparation procedure to remove interfering species by using dialysis membranes with molecular weight cut-offs higher than buffer species but lower than the analyte molecular weight. We showed that dialysis of PBS buffer significantly reduced the signal to manageable levels (**Figure S9**). Centrifugal desalting columns and microwell spin plates could alternatively be used for a faster and high-throughput sample pre-treatment process. We also conducted additional selectivity test with Bovine Serum Albumin

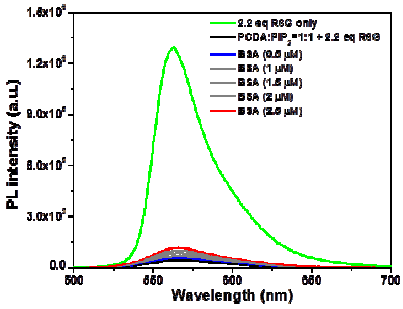


**Figure 4.** Changes in PL spectra of PCDA/$PIP_2$/R6G liposome solution as various concentration of BSA is added.

(BSA) protein that contains cationic 59 lysine residues. However, BSA did not induce significant false signal even at very high concentrations (2.5 μM) compared to the detection limit (2.3 nM) of neomycin, indicating that our system has sufficient selectivity to be used as a sensory platform for real-life applications (**Figure 4**). The presented sensory platform has several merits: high sensitivity, readily applicable to other sensor designs, and conveniently compatible with conventional 96-well plates and microplate readers used for ELISA.

## Conclusions

We developed a novel liposome-based fluorescence turn-on sensing platform by assembling R6G to a H-type aggregation on phospholipid-liposome surfaces. The H-aggregation and consequent fluorescence quenching were driven by Coulombic interaction between R6G and phospholipids and hydrophobic interaction of the dyes. Co-assembly of PCDA with the receptor-linked phospholipids ($PIP_2$) into liposomes rendered largely enhanced stability to the formed liposomes via photopolymerizaton of PCDA. Rationally devised displacement of the R6G aggregates at the phospholipid-liposome surface by target analytes driven by the specific interaction between receptors and analytes releases R6G dyes from the aggregates, producing a bright fluorescence turn-on signal. As a validation, highly selective and sensitive neomycin detection down to 2.3 nM was demonstrated. This new sensory platform can be readily applicable to other sensor designs and compatible with conventional 96-well plates and microplate readers for ELISA.

## Notes and references

[a] *Macromolecular Sci. and Eng.,* [b]*Materials Sci. and Eng.,* [c]*Chemical Eng.,*[d]*Biomedical Eng., and* [e]*Chemistry, University of Michigan*
*E-mail: jinsang@umich.edu*

† Electronic Supplementary Information (ESI) available: [details of any supplementary information available should be included here]. See DOI: 10.1039/b000000x/

‡ S. Seo, M. S. Kwon, A. Phillips contributed equally to this work. We acknowledge the financial support from Animal, Plant and Fisheries Quarantine and Inspection Agency of Korea (I-AD14-2011-13-11) and the Converging Research Center Program funded by the Ministry of Science, ICT and Future Planning (Project No. 2013K000314).

1 S. Mura, J. Nicolas, P. Couvreur, *Nat. Mater.* 2013, **12**, 991.
2 D. Peer, J. M. Karp, S. Hong, O. C. Farokhzad, R. Margalit, R. Langer, R. *Nat. Nanotechnol.* 2007, **2**, 751.
3 K, Raemdonck, K. Braeckmans, J. Demeester, S. C. De Smedt, *Chem. Soc. Rev.* 2014, **43**, 444.
4 M. Bally, K. Bailey, K. Sugihara, D. Grieshaber, J. Vörös, B. Städler, *Small* 2010, **6**, 2481.
5 A. Jesorka, O. Orwar, *Annu. Rev. Anal. Chem.* 2008, **1**, 801.
6 Y. K. Lee, H. Lee, J. -M. Nam, *NPG Asia Mater* 2013, **5**, 48
7 N. Dave, J. Liu, J. *Adv. Mater.* 2011, **23**, 3182.
8 L. S. Jung, J. S. Shumaker-Parry, C. T. Campbell, S. S. Yee, M. H. Gelb, *J. Am. Chem. Soc.* 2000, **122**, 4177.
9 K. W. Y. Chan, G. Liu, X. Song, H. Kim, T. Yu, D. R. Arifin, A. A. Gilad, J. Hanes, P. Walczak, P. C. M. van Zijl, J. W. M. Bulte, M. T. McMahon, *Nat. Mater.* 2013, **12**, 268.
10 K. A. Edwards, A. J. Baeumner, *Anal. Chem.* 2007, **79**, 1806.
11 F. Patolsky, A. Lichtenstein, I. Willner, *J. Am. Chem. Soc.* 2001, **123**, 5194.
12 J. Zhou, Q. -X. Wang, C. -Y. Zhang, *J. Am. Chem. Soc.* 2013, **135**, 2056.
13 K. Y. Chumbimuni-Torres, J. Wu, C. Clawson, M. Galik, A. Walter, G. -U. Flechsig, E. Bakker, L. Zhang, J. Wang, *Analyst* 2010, **135**, 1618.
14 R. Gui, A. Wan, X. Liu, H. Jin, *Chem. Commun.* 2014, **50**, 1546.
15 J. Ruiz, F. M. Goni, A. Alonso, *Biochim. Biophys. Acta.* 1988, **937**, 127.
16 Y. Wang, K. Zhou, G. Huang, C. Hensley, X. Huang, X. Ma, T. Zhao, B. D. Sumer, R. J. DeBerardinis, J. Gao, *Nat. Mater.* 2013, **13**, 204.
17 X. Yue, C. Guo, Y. Jing, F. Ma, *Analyst* 2012, **137**, 2027.
18 X. Chen, G. Zhou, X. Peng, J. Yoon, *Chem. Soc. Rev.* 2012, **41**, 4610.
19 X. Sun, T. Chen, S. Huang, L. Li, H. Peng, *Chem. Soc. Rev.* 2010, **39**, 4244.
20 D. J. Anh, J. M. Kim, *Acc. Chem. Res.* 2008, **41**, 805.
21 S. Seo, J. Lee, E. J. Choi, E. J. Kim, J. Y. Song, J. Kim, *Macromol. Rapid. Commun.* 2013, **34**, 743.
22 J. Lee, H. J. Kim, J. Kim, *J. Am. Chem. Soc.* 2008, **130**, 5010.
23 J. Lee, H. Jun, J. Kim, *Adv. Mater.* 2009, **21**, 3674.
24 D. H. Charych, J. O. Nagy, W. Spevak, M. D. Bdenarski, *Science*, 1993, **262**, 585.
25 M. Lofaj, I. Valent, J. Bujdák, *Cent. Eur. J. Chem.* 2013, **11**, 1606.
26 M. Ogawa, N. Kosaka, P. L. Choyke, H. Kobayashi, *ACS Chem. Bio.* 2009, **4**, 535.
27 M. Fischer, J. Georges, *Spectrochim. Acta. A* 1997, **53**, 1419.
28 R. Halterman, J. Moore, W. Yip, *J. Fluoresc.* 2011, **21**, 1467.
29 J. T. Buboltz, G. W. Feigenson, *Langmuir* 2005, **21**, 6296.
30 V. K. Kelkar, B. S. Valalulikar, J. T. Kunjappu, C. Manohar, *Photochem. Photobiol.* 1990, **52**, 717.
31 J. C. Mialocq, P. Hebert, X. Armand, R. Bonneau, J. P. J. Morand, *Photochem. Photobiol*. A 1991, **56**, 323.
32 M. D. Deumie, P. Lorente, D. Morizon, *Photochem. Photobiol. A* 1995, **89**, 239.
33 F. L. Arbeloa, M. J. T. Estevez, T. L. Arbeloa, I. L. Arbeloa, *Langmuir* 1995, **11**, 3211.
34 C. Nasr, D. Liu, S. Hotchandani, P. V. Kamat, *J. Phys. Chem.* 1996, **100**, 11054.
35 D. Avnir, D. Levy, R. Reisfeld, *J. Phys. Chem.* 1984, **88**, 5956.
36 I. S. Lim, F. Goroleski, D. Mott, N. Kariuki, W. Ip, J. Luo, C. Zhong, *J. Phys. Chem. B* 2006, **110**, 6673.
37 N. Narband, M. Uppal, C. W. Dunnill, G. Hyett, M. Wilson, I. P. Parkin, *Phys. Chem. Chem. Phys.* 2009, **11**, 10513.
38 K. Kalyanasundaram, J. K. Thomas, *J. Am. Chem. Soc.* 1977, **99**, 2039.
39 C. -C. You, O. R. Miranda, B. Gider, P. S. Ghosh, I. -B. Kim, B. Erdogan, S. A. Krovi, U. H. F. Bunz, V. M. Rotello, *Nat. Nanotechnol.* 2007, **2**, 318.
40 B. Mu, J. Zhang, T. P. McNicholas, N. F. Reuel, S. Kruss, M. S. Strano, *Acc. Chem. Res.* 2014, **47**, 979.
41 D. H. Kang, H. -S. Jung, N. Ahn, J. Lee, S. Seo, K. -Y. Suh, J. Kim, K. Kim, *Chem. Commun.* 2012, **48**, 5313.
42 D. H. Kang, H. -S. Jung, J. Lee, S. Seo, J. Kim, K. Kim, K. -Y. Suh, *Langmuir* 2012, **28**, 7551.
43 S. Nawaz, A. Kippert, A. S. Saab, H. B. Werner, T. Lang, K. -A. Nave, M. Simons, *J. Neurosci.* 2009, **29**, 4794.
44 The limit of detection (LOD) calculated from S/N = 3 ratio was found to be 2.3 nM at concentration range from 10 nM to 50 nM. The original PL spectra were shown in Figure S6.
45 L. A. A. Rooijen, B. W. Agranoff, *Neurochem Res* 1985, **10**, 1019.
46 S. Au, N. D. Weiner, J. Schacht, *Biochimica et Biophysica Acta (BBA) - Biomembranes* 1987, **902**, 80.

Herein, we report our systematic approach to develop a novel turn-on type liposome-based sensing platform by assembling fluorescence dyes to form H-type aggregation with efficient emission quenching on phospholipid-liposome surfaces. Rationally devised specific interactions between the phospholipid and a target analyte effectively release the fluorescence dyes from H-aggregate, producing a bright fluorescence turn-on signal. As a demonstration, such a sensory system for neomycin detection with very high sensitivity down to 2.3 nM was demonstrated, which is one of the most sensitive detection limits of neomycin among liposome-based sensors.

**Highly Sensitive Turn-on Biosensors by Regulating Fluorescence Dye Assembly on Liposome Surfaces**